tvst

Article

Wide-Field Swept-Source Optical Coherence Tomography Angiography Analysis of the Periarterial Capillary-Free Zone in Branch Retinal Vein Occlusion

Wenyi Tang[1–4,*], Jingli Guo[1–4,*], Xiaonan Zhuang[1–4], Ting Zhang[1–4], Ling Wang[1–4], Keyan Wang[1–4], Qing Chang[1–4], Wei Liu[1–4], and Gezhi Xu[1–4]

[1] Department of Ophthalmology, Eye and ENT Hospital of Fudan University, Shanghai, China
[2] Shanghai Key Laboratory of Visual Impairment and Restoration, Fudan University, Shanghai, China
[3] NHC Key Laboratory of Myopia, Fudan University, Shanghai, China
[4] Laboratory of Myopia, Chinese Academy of Medical Sciences, Shanghai, China

Correspondence: Wei Liu, Department of Ophthalmology, Eye and ENT Hospital of Fudan University, 83 Fenyang Road, Shanghai 200031, China. e-mail: bfgf2020@163.com
Qing Chang, Department of Ophthalmology, Eye and ENT Hospital of Fudan University, 83 Fenyang Road, Shanghai 200031, China. e-mail: qngchang@aliyun.com

Received: September 21, 2020
Accepted: January 3, 2021
Published: February 10, 2021

Keywords: Branch retinal vein occlusion; swept-source optical coherence tomography angiography; periarterial capillary free zone; visual function; retinal ischemia

Citation: Tang W, Guo J, Zhuang X, Zhang T, Wang L, Wang K, Chang Q, Liu W, Xu G. Wide-field swept-source optical coherence tomography angiography analysis of the periarterial capillary-free zone in branch retinal vein occlusion. Trans Vis Sci Tech. 2021;10(2):9, https://doi.org/10.1167/tvst.10.2.9

Purpose: To investigate the characteristics of the retinal periarterial capillary-free zone (paCFZ) with wide-field swept-source optical coherence tomography angiography (SS-OCTA) in eyes with branch retinal vein occlusion (BRVO).

Methods: Seventy treatment-naïve eyes with BRVO and 35 healthy eyes were included. The paCFZ areas, artery calibers, and areas of the major arteries in the unaffected quadrants of BRVO eyes were measured in 12 × 12-mm SS-OCTA images and compared with those of the contralateral eyes and healthy eyes. Other multimodal imaging data were collected.

Results: There were no significant differences in the unaffected artery caliber or area among the three groups (all $P > 0.05$). The unaffected paCFZ areas and the ratios of the unaffected paCFZ area to the counterpart artery area (paCFZ/artery area) of the major arteries were significantly larger than those in the contralateral or healthy eyes (all $P < 0.05$). Subgroup analysis revealed that the paCFZ/artery area value differed significantly between ischemic and nonischemic BRVO eyes ($P < 0.01$). The paCFZ/artery area value was positively correlated with logMAR best-corrected visual acuity, symptom duration, central macular thickness, and retinal nonperfusion area in BRVO.

Conclusions: Quantitative SS-OCTA measurements confirmed enlarged paCFZs along the unaffected major retinal arteries in BRVO eyes. The paCFZ parameters were correlated with symptom duration, retinal ischemia, and visual function.

Translational Relevance: Retinal periarterial capillary-free zones in BRVO can be noninvasively measured by SS-OCTA, assisting in clinically identifying retinal ischemia and evaluating visual function.

Introduction

Branch retinal vein occlusion (BRVO) is one of the most common retinal vascular diseases and an important cause of visual impairment worldwide.[1] Retinal vein occlusion reduces blood flow to the affected area of the retina, which can result in an increased area of retinal nonperfusion (RNP) and hypoxia.[2] Hypoxia, in turn, causes an increase in the expression of

vascular endothelial growth factor (VEGF) and accelerates the development of macular edema and retinal neovascularization,[3,4] greatly influencing the prognosis and visual outcome.

The periarterial capillary-free zone (paCFZ) is an area of physiological avascularization surrounding the retinal arteries in which no efferent vessels emerge directly from the walls.[5] It was first identified by His in 1880[6] and is thought to develop during embryogenesis along human retinal arteries confined to the plane of the superficial plexus.[7] As the transmural oxygen diffusion from the retinal artery can meet the metabolic demands of the nearby cells, the need for vessels in this area is mitigated, and the paCFZ develops. The paCFZ may expand or converge in concert with changes in the retinal oxygen saturation in many retinal vascular disorders and is an important indirect index of the intravascular oxygen partial pressure.[8,9] Histological studies of the paCFZ have been conducted in human donor eyes,[5,10] but the evaluation of the paCFZ in living human eyes has been limited, even with conventional fluorescein angiography, because the resolution achieved is inadequate.

Optical coherence tomography angiography (OCTA) can visualize the retinal vessels without recourse to dye injections.[11] With the development of OCTA software, the paCFZ can now be mapped with noninvasive methods and quantitatively measured.[12] Spectral-domain OCTA (SD-OCTA) has shown that the paCFZ is significantly larger and wider in severe nonproliferative diabetic retinopathy (DR) than in the healthy retina, indicating the usefulness of the paCFZ in monitoring the occurrence and progression of DR.[13] A recently developed swept-source OCTA (SS-OCTA) instrument (PLEX Elite 9000; Carl Zeiss Meditec, Oberkochen, Germany) that uses a longer and deeper penetrating central wavelength (1050 nm) can visualize retinal vasculature in large scan areas of 12 × 12 mm^2.[14,15] With widefield SS-OCTA, the periphery of the retina beyond the macula can be visualized well.

Until now, there have been few studies of the characteristics of the paCFZ and the changes in BRVO that have been demonstrated to show retinal oxygen saturation fluctuations.[16–18] The aims of this study were to qualitatively and quantitatively analyze the features of the paCFZ, as visualized with widefield SS-OCTA, in patients with BRVO and to investigate the clinical relevance of these features. Assessments of paCFZ and arterial parameters in the quadrant affected by occluded venules in BRVO eyes with SS-OCTA may be limited and unreliable because of the shadowing effect and signal attenuation caused by intraretinal hemorrhage and edema. Therefore, we analyzed paCFZ and artery parameters in the unaffected temporal quadrant.

Methods

Subjects and Examination

This observational, cross-sectional study included 70 treatment-naïve patients (70 eyes) who were diagnosed with unilateral BRVO at the Eye and ENT Hospital of Fudan University, Shanghai, China, between January 2019 and June 2020. Thirty-five volunteers (35 eyes) with no retinal disorders were also recruited. The study was approved by the institutional review board of the Eye and ENT Hospital of Fudan University and adhered to the tenets of the Declaration of Helsinki. All of the subjects provided written informed consent for the procedures.

All of the patients underwent a complete ophthalmic examination, including best-corrected visual acuity (BCVA) measurement (expressed as Snellen visual acuity ratios), intraocular pressure (IOP) measurement, automatic refractometry (Auto Refractometer RM-8900; Topcon, Inc., Tokyo, Japan), slit-lamp biomicroscopic examination, ultra-widefield fundus photography and fluorescein angiography (FFA) (Optos 200Tx; Optos PLC, Dunfermline, UK), and SD-OCT (Spectralis OCT; Heidelberg Engineering, Heidelberg, Germany). Fovea-centered OCTA scans of regions 12 × 12 mm^2 and 3 × 3 mm^2 were performed with an SS-OCTA PLEX Elite 9000 instrument (Carl Zeiss Meditec) between 09:00 and 11:00. The SS-OCTA instrument operated at an A-scan rate of 100,000 Hz, with lateral and axial resolutions of 20 µm and 6.3 µm, respectively. Each 12 × 12-mm or 3 × 3 volume consisted of 500 A-scans per B-scan and 500 B-scan locations per volume scan. Two repeated B-scans were acquired at each B-scan position to produce the OCTA images. The diagnosis of BRVO was based on criteria that included dot-like, blot-shaped, or flame-shaped intraretinal hemorrhages in a quadrant of the retina caused by the occlusion of one of the major branch veins; retinal edema with exudates; tortuosity and dilatation of the occluded veins; and FFA features such as delayed filling of the veins and macular edema and ischemia.[19] Ischemic BRVO was defined as a capillary nonperfusion area of >5 disk diameters (DDs) on FFA and nonischemic BRVO was defined as a capillary nonperfusion area of ≤ 5 DD.[20] Patients with the following characteristics were excluded: (1) other concurrent retinal diseases, such as DR or age-related macular degeneration; (2) a history of vitrectomy or intraocular therapy for BRVO,

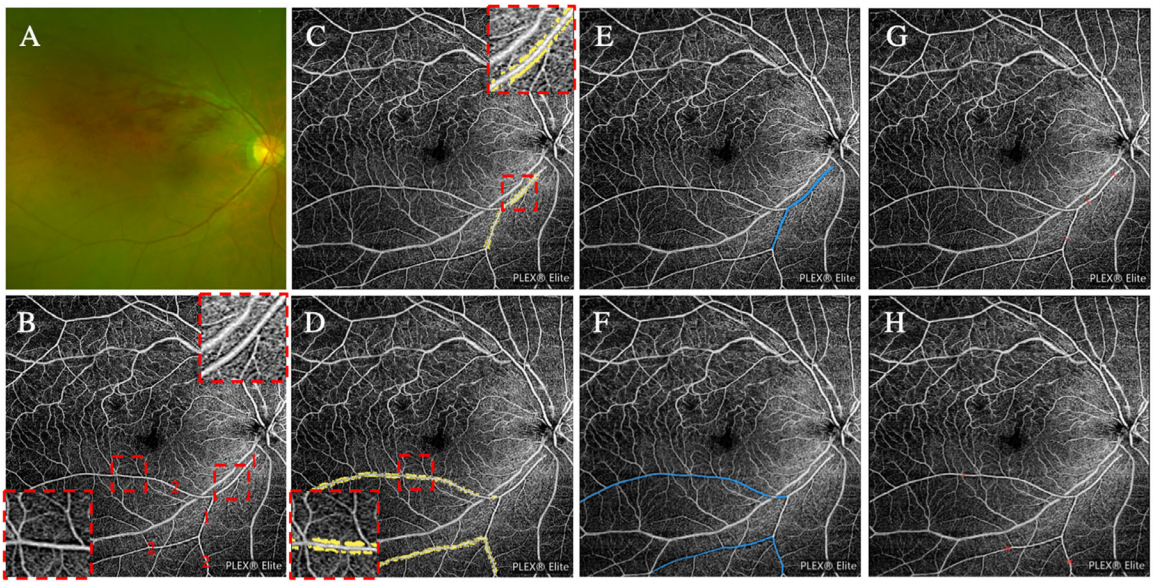

Figure 1. The schema for measurement of the paCFZ area, artery area, and artery caliber in the unaffected quadrant of BRVO eyes. (**A**) Color fundus photograph of the right eye from a 60-year-old male showing flame-shaped intraretinal hemorrhages in the superotemporal quadrant of the retina. The vessel order determination was made in the inferotemporal quadrant of the retina. (**B**) The corresponding 12 × 12-mm en face SS-OCTA images of the superficial capillary plexus extending from the inner limiting membrane to the inner plexiform layer. The numbers 1 and 2 represent a first-order artery and a second-order artery, respectively. The representative images of paCFZ along the first- and second-order arteries are shown in the magnified squares. Note that the perivenous capillary-free zone was less wide and prominent than the paCFZ of the same order. (**C**) The *yellow* area indicates the total paCFZ area in the first-order artery with a value of 0.38 mm^2. The magnified square shows the measurement details of the paCFZ area. (**D**) The *yellow* areas indicate the paCFZ areas in the second-order artery with a total value of 1.24 mm^2. The magnified square shows the measurement details of the paCFZ area. (**E**) The *blue* area indicates the first-order artery area with a value of 0.36 mm^2. (**F**) The *blue* area indicates the second-order artery area with a total value of 0.82 mm^2. (G, H) Three locations of the same order of the artery were chosen and two seed points (*red markers*) were added at each location. The distance between the seed points was calculated as the artery caliber, and the values were averaged for the same order of the artery. (**G**) First-order artery; (**H**) second-order artery.

including laser photocoagulation and intravitreal injection; (3) uncontrolled hypertension (blood pressure > 160/100 mm Hg) or cardiovascular or cerebrovascular disease; (4) a history of glaucoma or IOP ≥ 22 mm Hg; (5) high myopia (<−6.0 diopters), high hyperopia (>+5.0 diopters), or a history of refractive operation; or (6) cataract or other media opacities causing poor fundus images. The contralateral eyes of these patients were also carefully examined to exclude evidence of vascular occlusion or other coexisting retinal pathologies and confirm they were unaffected by BRVO. The control group was comprised of 35 subjects with a BCVA of 20/20 or better. One eye was randomly selected for each subject in the control group. They had no history of any ocular disease or surgery and unremarkable findings on the ophthalmic examinations.

Measurement of the paCFZ and Related Parameters

The customized, semiautomatic software Medraw (Image Medraw Technology Co., Ltd., Shanghai, China) was developed to measure the paCFZ area, artery caliber, and area of the major arteries (first- and second-order) in the unaffected quadrants of the BRVO eyes, the corresponding quadrants of the contralateral eyes, and the healthy control eyes on 12 × 12-mm^2 SS-OCTA images of the superficial retinal layer. The paCFZ area was defined as the contiguous region of low signal along the retinal artery, indicating a lack of microvasculature. To measure the paCFZ area and the artery area, the algorithm involved three steps. First, two independent graders (WT and JG) viewed the fundus photographs and SS-OCTA images simultaneously, and the first- and second-order arteries were identified, as previously reported.[21] After a seed point was added manually to the paCFZ or the corresponding artery by the grader, the software detected the pixel of the seed point, and the region nearby containing pixels between 0 and the pixel of the seed point was traced automatically. Second, the area of the traced paCFZ or the corresponding artery was calculated automatically in pixels (AreaPix) and then converted to square millimeters with the following formula: Area = AreaPix × [(realW × realH)/(pixW

Table 1. Characteristics of Patients with BRVO and Healthy Control Participants in This Study

Variables	BRVO Eyes ($n = 70$)	Fellow Eyes ($n = 70$)	Healthy Control Eyes ($n = 35$)	*P* (BRVO vs. Fellow)	*P* (Fellow vs. Control)
Age (y), mean ± SD	57.40 ± 9.41		56.80 ± 11.45	NA	0.80
Gender (men/women), *n*	38/32		18/17	NA	0.78
Right eye, *n* (%)	42 (60.0)	42 (60.0)	16 (45.7)	NA	0.17
Symptom duration (mo), mean ± SD	1.71 ± 1.37	NA	NA	NA	NA
IOP (mm Hg), mean ± SD	14.86 ± 3.42	15.40 ± 2.87	15.47 ± 2.85	0.27	0.92
Refractive error (SE, D), mean ± SD	−0.32 ± 1.46	−0.54 ± 1.57	−0.24 ± 1.18	0.16	0.37
Systolic blood pressure (mm Hg), mean ± SD	133.24 ± 11.62		128.24 ± 11.12	NA	0.06
Diastolic blood pressure (mmHg), mean ± SD	79.30 ± 7.62		79.45 ± 5.48	NA	0.92
Occlusion area (ST/IT), *n*	50/20	NA	NA	NA	NA
Quadrants measured (ST/IT), *n*	20/50	20/50	9/26	NA	0.76
BCVA (logMAR)	0.68 ± 0.35	0.01 ± 0.05	−0.00 ± 0.01	<0.01	0.20
BCVA (Snellen equivalent), mean (range)	20/32 (20/400–20/25)	20/20 (20/25–20/13)	20/20 (20/20–20/17)	NA	NA
VD of SCP (%), mean ± SD	38.97 ± 4.46	51.06 ± 4.08	52.62 ± 2.80	<0.01	0.07
VD of DCP (%), mean ± SD	35.88 ± 5.63	48.03 ± 6.56	50.24 ± 3.36	<0.01	0.09
FAZ of SCP (mm^2), mean ± SD	0.42 ± 0.17	0.36 ± 0.10	0.32 ± 0.09	<0.01	0.05
FAZ of DCP (mm^2), mean ± SD	1.10 ± 0.30	0.78 ± 0.21	0.80 ± 0.21	<0.01	0.71
CMT (μm), mean ± SD	570.98 ± 165.87	252.02 ± 17.43	257.00 ± 23.92	<0.01	0.29
SFCT (μm), mean ± SD	265.28 ± 69.74	258.57 ± 66.36	264.66 ± 44.07	0.31	0.66
Type (ischemia/nonischemia), *n*	44/26	NA	NA	NA	NA
RNP (mm^2), mean ± SD	42.59 ± 37.21	NA	NA	NA	NA

SE, spherical equivalent; D, diopter; ST, superotemporal; IT, inferotemporal; NA, not applicable.

Table 2. Measurements in Patients with BRVO and Healthy Control Participants

Variables	Mean ± SD			*P*	
	BRVO Eyes ($n = 70$)	Fellow Eyes ($n = 70$)	Healthy Control Eyes ($n = 35$)	BRVO vs. Fellow	Fellow vs. Control
First-order arteries					
Artery caliber (μm)	93.19 ± 13.05	93.50 ± 13.36	94.12 ± 16.08	0.86	0.85
Artery area (mm^2)	0.48 ± 0.19	0.50 ± 0.15	0.51 ± 0.15	0.23	0.97
paCFZ (mm^2)	0.56 ± 0.22	0.42 ± 0.13	0.43 ± 0.15	<0.01	0.78
paCFZ/artery area	1.19 ± 0.27	0.83 ± 0.22	0.83 ± 0.16	<0.01	0.91
Second-order arteries					
Artery caliber (μm)	60.73 ± 7.70	61.07 ± 8.69	62.43 ± 9.40	0.79	0.51
Artery area (mm^2)	0.60 ± 0.29	0.65 ± 0.22	0.64 ± 0.24	0.20	0.87
paCFZ (mm^2)	1.02 ± 0.52	0.74 ± 0.27	0.71 ± 0.26	<0.01	0.64
paCFZ/artery area	1.75 ± 0.54	1.17 ± 0.28	1.14 ± 0.29	<0.01	0.70

× pixH)]. The real width (realW), real height (realH), pixel width (pixW), and pixel height (pixH) of the 12 × 12-mm^2 SS-OCTA images were 12 mm, 12 mm, 1024 pixels, and 1024 pixels, respectively. Third, the graders reviewed and manually corrected the automatic demarcation as needed by deleting or adding the automatically demarcated regions of the paCFZ and the corresponding arteries. To measure the artery caliber, three locations of the same order of the artery were chosen and the values were averaged. The workflow for this software is presented in Figure 1.

Multimodal Imaging Analysis

Vascular density was defined as the proportion of pixels contributing to the blood flow signals over the whole area in thresholded OCTA images as previously reported.[22] The macular vascular density (VD) and foveal avascular zone (FAZ) of the superficial capillary plexus (SCP) and deep capillary plexus (DCP) on the 3 × 3-mm^2 SS-OCTA images were measured with the analysis tools in Fiji ImageJ (National Institutes of Health, Bethesda, MD), as previously described.[23,24] We used only SS-OCTA images with a signal strength of ≥7 and without obvious projection artifact or motion artifact that was identified by horizontal misalignment of vessel segments. Manual adjustments were made if uncorrected automatic segmentation occurred. The central macular thickness (CMT) and the subfoveal choroidal thickness (SFCT) were measured with the Heidelberg Spectralis software as previously described.[25,26] Briefly, the CMT was automatically measured in the 1-mm-diameter central region of the macular thickness map centered on the fovea, and the SFCT was measured with the enhanced-depth imaging modality from the inferior limit of the retinal pigment epithelium to the sclerachoroidal interface. The RNP was measured on ultra-widefield FFA images obtained 120 seconds after dye injection using ImageJ, as previously reported.[14] Two observers (WT and JG) performed all measurements independently and the average of the measurements was used for the analyses.

Statistical Analysis

BCVA values were converted into logarithm of the minimum angle of resolution (logMAR) values for statistical analysis. Continuous variables are presented as means ± standard deviations (SDs). The sample was calculated at the level of $\alpha = 0.05$ (two-sided) and $1 - \beta = 0.9$ using PASS software (Turntech, Beijing, China). The minimal estimated sample size was 32 for each group according to the preliminary test. Quantitative variables were compared between the BRVO and contralateral eyes with paired *t*-tests and between the contralateral eyes and healthy control eyes with unpaired *t*-tests. The χ^2 test was used for categorical variables. Univariate and multivariate linear regression analyses were made to determine the clinical factors associated with paCFZ parameters. Variables with $P < 0.05$ in the univariate analyses were included in the multivariate models using a stepwise method. Intraclass correlation (ICC) and coefficient of repeatability and reproducibility were used to assess repeatability and reproducibility.[27,28] The coefficient of repeatability was defined as 2 × SDs of the differences between pairs of measurements in the same subjects acquired during the same visit by the same observer divided by the average of the means of each pair of readings.[29]

Table 3. Comparison of Artery and paCFZ Parameters in the First- and Second-Order Arteries and OCTA Macular Metrics in the Affected Eyes Between Ischemic and Nonischemic BRVO

	BRVO, Mean ± SD		
Variables	Ischemic ($n = 44$)	Nonischemic ($n = 26$)	P
First-order arteries			
Artery caliber (µm)	91.75 ± 13.41	93.30 ± 12.14	0.68
Artery area (mm^2)	0.45 ± 0.18	0.53 ± 0.20	0.15
paCFZ (mm^2)	0.56 ± 0.23	0.55 ± 0.26	0.88
paCFZ/artery area	1.29 ± 0.24	1.05 ± 0.25	<0.01
Second-order arteries			
Artery caliber (µm)	60.85 ± 7.71	61.72 ± 8.40	0.71
Artery area (mm^2)	0.60 ± 0.32	0.60 ± 0.26	0.97
paCFZ (mm^2)	1.17 ± 0.76	0.91 ± 0.45	0.17
paCFZ/artery area	1.91 ± 0.54	1.50 ± 0.45	<0.01
VD of SCP (%)	38.67 ± 4.18	39.41 ± 4.93	0.57
VD of DCP (%)	36.67 ± 6.21	34.69 ± 4.53	0.23
FAZ of SCP (mm^2)	0.42 ± 0.17	0.43 ± 0.16	0.81
FAZ of DCP (mm^2)	1.09 ± 0.26	1.122 ± 0.36	0.74

The coefficient of reproducibility was defined as 2 × SDs of the difference between measurements acquired from the repetition of the scans by different observers divided by the average response.[29] $P < 0.05$ was considered statistically significant. SPSS Statistics 21 (IBM, Armonk, NY) was used for all statistical analyses.

Results

Seventy treatment-naïve eyes of 70 patients were included. Twenty-five patients (35.7%) had a history of arterial hypertension. The control group consisted of 35 individuals. Eight patients (22.8%) had a history of arterial hypertension. There were no significant differences between the BRVO group and the control group regarding age, sex, ocular dominance ratio, IOP, refractive error, systolic and diastolic blood pressure, or the quadrants measured (all $P > 0.05$) (Table 1).

The BRVO eyes had worse logMAR BCVA, lower microvascular densities of the SCP and DCP, larger superficial and deep FAZs, and a thicker CMT than the contralateral eyes (all $P < 0.01$). Forty-four patients had ischemic BRVO and 26 nonischemic BRVO. There were no significant differences in logMAR BCVA, the VDs of SCP or DCP, superficial or deep FAZs, CMT, SFCT, or the paCFZ quadrants between the contralateral eyes and the healthy control eyes (all $P > 0.05$) (Table 1).

The mean calibers and areas of the first-order and second-order arteries in the unaffected quadrant did not differ among the BRVO eyes, contralateral eyes, and healthy control eyes (all $P > 0.05$) (Table 2). Because the paCFZ was not symmetrically or evenly distributed along the arteries, when detected with SS-OCTA, the paCFZ area was measured and summed along each order of retinal arteries. For the first-order and second-order arteries, the mean paCFZ area and the ratio of the paCFZ area to the artery area were significantly larger in the BRVO eyes than in the contralateral eyes (all $P < 0.01$), respectively (Table 2, Fig. 2). Neither of these two parameters differed significantly between the contralateral eyes and the healthy control eyes (all $P > 0.05$) (Table 2). The high ICC values demonstrated excellent agreement between measurements, and the coefficients of repeatability and reproducibility indicated high intra-observer repeatability and inter-observer reproducibility for all the measured data (Supplementary Tables S1–S3). Also, there was no significant difference between the superior temporal and inferior temporal measurements of paCFZ, artery area and caliber, and the ratio of paCFZ area to artery area (Supplementary Table S4).

A subgroup analysis demonstrated that the ratios of the paCFZ area to the artery area for the first- and second-order arteries were significantly larger in the eyes with ischemic BRVO than in those with nonischemic BRVO, whereas the corresponding artery calibers, artery areas, paCFZ areas, and macular VD and FAZ areas of SCP and DCP were not significantly different between these two groups (Table 3). Univariate and multivariate linear regression analyses revealed that logMAR BCVA, symptom duration, CMT, and the area of RNP were significantly correlated with

Table 4. Analysis of Clinical Factors Associated with paCFZ Parameters in BRVO Patients

	First paCFZ/Artery Area						Second paCFZ/Artery Area					
	Univariate			Multivariate			Univariate			Multivariate		
Variables	β	95% CI	*P*	β	95% CI	*P*	β	95% CI	*P*	β	95% CI	*P*
Age	0.002	−0.007–1.576	0.694	—	—	—	−0.003	−0.028 to 0.023	0.841	—	—	—
Duration	0.084	0.033–0.135	0.002	0.062	0.023–0.101	0.003	0.267	0.113 to 0.421	0.001	0.132	0.026–0.239	0.016
IOP	−0.016	−0.038–0.007	0.163	—	—	—	−0.012	−0.081 to 0.056	0.717	—	—	—
SBP	−0.003	−0.009–0.004	0.432	—	—	—	−0.017	−0.037 to 0.003	0.087	—	—	—
DBP	−0.002	−0.013–0.008	0.625	—	—	—	−0.028	−0.058 to 0.002	0.068	—	—	—
BCVA	0.521	0.357–0.684	<0.001	0.300	0.127–0.472	0.001	1.447	0.915 to 1.980	<0.001	0.499	0.013–0.985	0.044
VD of SCP	−0.005	−0.023–0.012	0.526	—	—	—	−0.018	−0.071 to 0.035	0.493	—	—	—
VD of DCP	−0.002	−0.015–0.012	0.821	—	—	—	−0.025	−0.052 to 0.002	0.064	—	—	—
FAZ of SCP	0.162	−0.299–0.623	0.483	—	—	—	0.164	−1.248 to 1.577	0.816	—	—	—
FAZ of DCP	0.036	−0.220–0.292	0.780	—	—	—	−0.100	−0.882 to 0.682	0.897	—	—	—
CMT	0.001	0.000–0.001	<0.001	0.001	0–0.002	0.017	0.003	0.002 to 0.004	<0.001	0.002	0.001–0.003	<0.001
SFCT	0.000	−0.001–0.001	0.891	—	—	—	0.000	−0.003 to 0.004	0.898	—	—	—
RNP	0.003	0.001–0.005	0.002	0.002	0–0.003	0.036	0.012	0.007 to 0.017	<0.001	0.007	0.003–0.011	0.001

CI, confidence interval; first paCFZ/artery area, ratio of paCFZ area to artery area in the first-order retinal artery; second paCFZ/artery area, ratio of paCFZ area to artery area in the second-order retinal artery; SBP, systolic blood pressure; DBP, diastolic blood pressure.

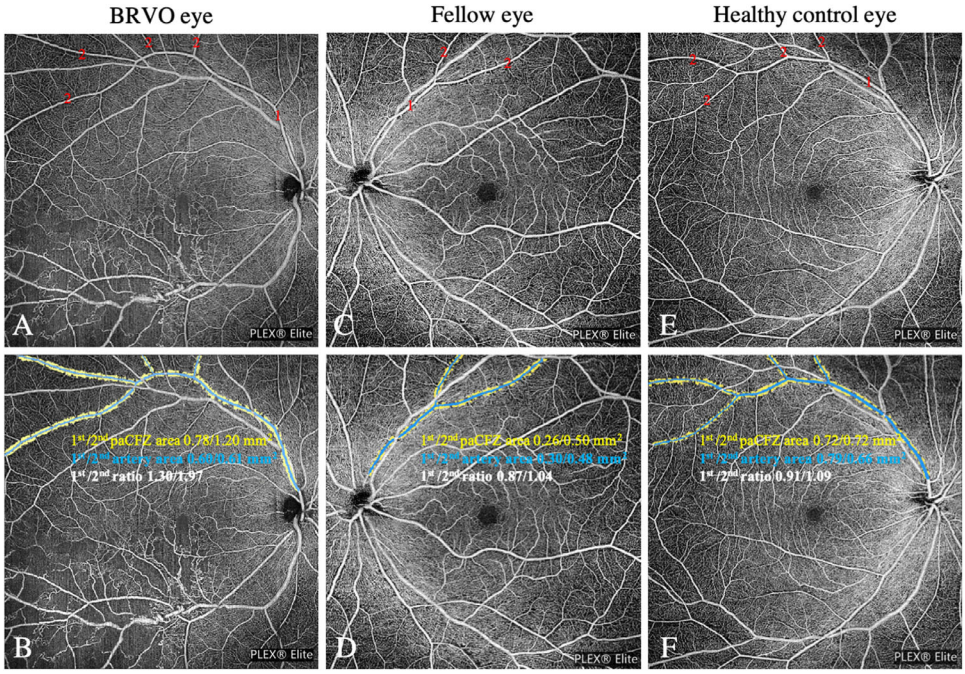

Figure 2. En face SS-OCTA images (12 × 12 mm) from a 56-year-old male patient (**A**–**D**) and an age- and sex-matched healthy participant (**E**, **F**). (**A**, **B**) The BRVO eye showed a large area of retinal nonperfusion in the affected inferotemporal quadrant of the retina. The first- and second-order arteries in the superotemporal quadrant were determined (**A**), and the corresponding paCFZ areas and artery areas were measured (**B**). The paCFZ areas along the first- and second-order arteries were 0.78 mm^2 and 1.20 mm^2, respectively. The areas of the first- and second-order arteries were 0.60 mm^2 and 0.61 mm^2, respectively. Consequently, the ratios of paCFZ area to artery area were 1.30 and 1.97, respectively. (**C**, **D**) The unaffected eye from the same patient. The paCFZ areas along the first- and second-order arteries were 0.26 mm^2 and 0.50 mm^2, respectively. The areas of the first- and second-order arteries were 0.30 mm^2 and 0.48 mm^2, respectively. Consequently, the ratios of paCFZ area to artery area were 0.87 and 1.04, respectively. (**E**, **F**) The control eye from an age- and sex-matched healthy participant. The paCFZ areas along the first- and second-order arteries were 0.72 mm^2 and 0.72 mm^2, respectively. The areas of the first- and second-order arteries were 0.79 mm^2 and 0.66 mm^2, respectively. Consequently, the ratios of paCFZ area to artery area were 0.91 and 1.09, respectively.

the ratios of the paCFZ areas to the artery areas in the first-order and second-order arteries, respectively (Table 4).

Discussion

In this study, we quantified the paCFZ area in different branches of the retinal arteries using a SS-OCTA device and compared the findings in eyes with BRVO with those in the contralateral eyes and in healthy control eyes. In eyes with BRVO, there were increases in the paCFZ area and the ratio of the paCFZ area to the artery area, and the latter was more pronounced in the ischemic type of BRVO. Other findings included a correlation between the ratio of the paCFZ area to the artery area and visual function. To our knowledge, this is the first study to quantify the paCFZ area in patients with BRVO relative to that in healthy individuals.

Previous studies have shown that the paCFZ is present in healthy subjects using histology, adaptive optics scanning laser ophthalmoscopy, and OCTA.[8,30,31] However, the measurements of the paCFZ varied between studies. In adult humans, the average width of the paCFZ was reported to be 50 µm posteriorly and 120 µm peripherally.[31] Using SD-OCTA, Arthur et al.[30] reported the width of the paCFZ to be 67.2 ± 25.3 µm. Mase et al.[8] measured the capillary-free zone (CFZ) area in a 0.5 × 0.5-mm^2 square and found that the average CFZ areas adjacent to the first- and second-order branches were 0.050 ± 0.007 mm^2 and 0.070 ± 0.009 mm^2, respectively. In contrast to those studies, we measured the paCFZ in a wider field of view (12 × 12 mm^2), and the mean paCFZ areas in the first- and second-order artery branches were 0.43 ± 0.15 mm^2 and 0.71 ± 0.26 mm^2, respectively. We also calculated the ratio of the paCFZ area to the artery area to reduce the impact of the variability in the retinal artery branches. The first- and second-order artery ratios were 0.83 ± 0.16 and 1.14 ± 0.29, respectively. Therefore, widefield SS-OCTA may be a useful tool for the accurate and detailed evaluation of the paCFZ.

Several hypotheses have been proposed to explain the pathogenesis of BRVO, including compression of the veins at arteriovenous crossings, degenerative changes within the venous walls, and hematological disorders.[32] Occlusion of a branch venule and a reduction in retinal oxygen consumption in the occluded area may lead to the increase in arterial oxygen saturation seen in BRVO eyes.[18] The formation of collaterals and shunting vessels can also increase the oxygen saturation in the unaffected arteries.[16,33] In this study, both the unaffected paCFZ area and the corresponding ratio of the paCFZ area to the artery area were significantly larger in BRVO eyes than those in the corresponding quadrants of the contralateral eyes, whereas they were similar between the contralateral eyes and the healthy eyes. We speculated that this was attributable to a change in the local conditions in the BRVO eyes. The paCFZ represents the maximum distance that oxygen and nutrients must diffuse to reach the retinal neurons and is closely related to the oxygen pressure in the retinal vessels. It is likely that the increased arterial oxygen saturation in BRVO leads to an increase in the diffusion distance of oxygen and thus an enlargement of the paCFZ. Meanwhile, the larger paCFZ may result from the potential ischemia of a very sick retina and the consequent reduced oxygen demand in BRVO eyes.[30]

BRVO can be categorized as ischemic or nonischemic, depending on the perfusion status.[34] Ischemic pathological changes can induce more capillary nonperfusion areas with the increased production of VEGF.[35] It has been suggested that high levels of VEGF cause capillary closure and worsening ischemia.[35] Although the paCFZ area in the unaffected first- and second-order arterial branches did not differ significantly between the two types of BRVO, the paCFZ area tended to be larger in the ischemic type. However, the arterial calibers and areas in the first- and second-order arterial branches did not differ between the ischemic and nonischemic types. It is possible that the walls of the arteries are thicker and more resistant to the vasodilatory effect of VEGF.[36,37] Surprisingly, the ratio of the paCFZ area to the artery area was significantly larger in the ischemic type of BRVO. This suggests that this parameter may be a more sensitive biomarker for distinguishing the different types of BRVO. The clinical significance needs be confirmed in future studies with larger samples.

A correlation analysis demonstrated that the ratio of the paCFZ area to the artery area correlated significantly with symptom duration, the size of the nonperfusion area, and the severity of macular edema (CMT). The longer duration of symptoms probably correlates with a longer period of vein occlusion and therefore a greater opportunity for the enlargement of the paCFZ. The retinal nonperfusion is created by the deterioration of retinal blood flow caused by occlusion of a retinal branch, the area of which over 5 DDs is classified as ischemic.[20] The intraocular VEGF level is presumably positively associated with the total retinal nonperfusion area.[35] A larger area of retinal nonperfusion may indicate a sicker retina with a reduced oxygen demand. It is also likely that a larger nonperfusion area contributes to higher VEGF levels and promotes capillary dropout around the arteries. Meanwhile, larger nonperfusion area may facilitate the formation of collaterals and shunting vessels[38] and thus increase the oxygen saturation in the unaffected arteries, which may lead to an enlarged paCFZ area. The reason for the association between the ratio and CMT is unclear. Greater CMT may indicate a greater breakdown of the blood–retinal barrier and higher levels of vasopermeability factors, such as VEGF.[39] Also, increased CMT may suggest severe macular edema and prolonged damage of neuronal cells in the retina,[40] which possibly result in a reduction of oxygen demand from neuronal cells and subsequently a larger paCFZ area. Finally, a larger ratio of paCFZ area to artery area is associated with worse BCVA. We hypothesize that it is partly attributable to the fact that the paCFZ parameter mirrors the microcirculation of the inner retina. Larger paCFZ parameter may reflect more severe global ischemia within the inner retina, including macula, which is likely to affect visual acuity.[41]

There are several advantages of the paCFZ biomarker. First, the microangiopathy of the inner retina can be at least partly reflected by the paCFZ parameters. This is different from the OCTA metrics regarding the macula and its surroundings such as FAZ area or vessel density. Second, the ratio of the paCFZ area to the artery area can be used as a more sensitive biomarker for distinguishing ischemic and non-ischemic BRVO. This is possibly because the ratio is calculated in a wider field of view on the basis of the global retinal circulatory status and less influenced by the macular edema or hemorrhage that may interfere with the measurement of OCTA macular metrics. Therefore, we suggest the paCFZ parameters be used either alone or in combination with macular metrics to evaluate the retinal ischemia of BRVO.

This study had several limitations. First, on the $12 \times 12\text{-mm}^2$ OCTA images centered on the fovea, the second-order vessels were not always included in the scan area; however, the ratio of the paCFZ area to the artery area might have reduced its impact. Second, in this study, we did not measure the perivenous CFZ, which is narrower and less promi-

nent than the paCFZ.[26,42] The changes in the perivenous CFZ during BRVO warrant further investigation. Third, because this was a cross-sectional study with a relatively small sample size, further longitudinal studies with larger sample sizes are required to clarify the potential dynamic changes in the paCFZ after treatment. Fourth, the OCTA examinations were not done at the same time, but there may be diurnal variations in OCTA parameters.[43] Fifth, the retinal arteriolar caliber may be related to blood pressure.[44] Although the arteriolar caliber in this study did not differ significantly, it should be considered when interpreting the results. Finally, ocular magnification errors from different axial lengths in individuals were not corrected due to a lack of axial length measurements. However, patients with a refractive error (spherical equivalent) over 5 diopter were excluded. As refractive error is believed to show the strongest correlation with axial length, this exclusion would place magnification errors within less than 15% for all the subjects.[45] Nevertheless, future studies using this software and SS-OCTA with image size correction for axial length and refractive error should be designed.

In summary, the ratio of the paCFZ area to the artery area was significantly larger in eyes with BRVO than in the contralateral eyes and correlated significantly with symptom duration, retinal ischemia, and visual acuity in eyes with BRVO. The paCFZ parameter can be used either alone or in combination with macular metrics to identify retinal ischemia and may be used as a biomarker in the classification and monitoring of BRVO.

Acknowledgments

Supported by grants from the National Natural Science Foundation of China (81700861, 81700862, 81770944, 81800846), Study on the Comprehensive Prevention and Control of Common Eye Diseases in Xuhui District (XHLHGG201807), Shanghai Hospital Development Center (SHDC12016116, SHDC2020CR2041B), and Science and Technology Commission of Shanghai Municipality (16411953700, 17411961900, 18411965100).

Disclosure: **W. Tang,** None; **J. Guo,** None; **X. Zhuang,** None; **T. Zhang,** None; **L. Wang,** None; **K. Wang,** None; **Q. Chang,** None; **W. Liu,** None; **G. Xu,** None

* WT and JG contributed equally to this article.

References

1. Rogers S, McIntosh RL, Cheung N, et al. The prevalence of retinal vein occlusion: pooled data from population studies from the United States, Europe, Asia, and Australia. *Ophthalmology.* 2010;117(2):313–319.
2. Stefansson E, Novack RL, Hatchell DL. Vitrectomy prevents retinal hypoxia in branch retinal vein occlusion. *Invest Ophthalmol Vis Sci.* 1990;31(2):284–289.
3. Noma H, Funatsu H, Yamasaki M, et al. Pathogenesis of macular edema with branch retinal vein occlusion and intraocular levels of vascular endothelial growth factor and interleukin-6. *Am J Ophthalmol.* 2005;140(2):256–261.
4. Ozaki H, Hayashi H, Vinores SA, Moromizato Y, Campochiaro PA, Oshima K. Intravitreal sustained release of VEGF causes retinal neovascularization in rabbits and breakdown of the blood-retinal barrier in rabbits and primates. *Exp Eye Res.* 1997;64(4):505–517.
5. Michaelson I, Campbell A. The anatomy of the finer retinal vessels, and some observations on their significance in certain retinal diseases. *Trans Ophthalmol Soc UK.* 1940;60:71–111.
6. His W. Abbildungen uber des Gefaszsystem der menschlichen Netzhaut und derjenigen des Kaninchens. *Arch f Anat u Entwickelungsg.* 1880;224–231.
7. Hughes S, Yang H, Chan-Ling T. Vascularization of the human fetal retina: roles of vasculogenesis and angiogenesis. *Invest Ophthalmol Vis Sci.* 2000;41(5):1217–1228.
8. Mase T, Ishibazawa A, Nagaoka T, Yokota H, Yoshida A. Radial peripapillary capillary network visualized using wide-field montage optical coherence tomography angiography. *Invest Ophthalmol Vis Sci.* 2016;57(9):OCT504–OCT510.
9. Phelps DL. Oxygen and developmental retinal capillary remodeling in the kitten. *Invest Ophthalmol Vis Sci.* 1990;31(10):2194–2200.
10. Balaratnasingam C, An D, Sakurada Y, et al. Comparisons between histology and optical coherence tomography angiography of the periarterial capillary-free zone. *Am J Ophthalmol.* 2018;189:55–64.
11. Kashani AH, Chen CL, Gahm JK, et al. Optical coherence tomography angiography: a comprehensive review of current methods and clinical applications. *Prog Retin Eye Res.* 2017;60:66–100.

12. Muraoka Y, Uji A, Ishikura M, Iida Y, Ooto S, Tsujikawa A. Segmentation of the four-layered retinal vasculature using high-resolution optical coherence tomography angiography reveals the microcirculation unit. *Invest Ophthalmol Vis Sci.* 2018;59(15):5847–5853.
13. Li H, Ding X, Lu L, Yang J, Ma J. Morphometry of the normal retinal periarterial capillary-free zone and changes during severe nonproliferative diabetic retinopathy. *Clin Hemorheol Microcirc.* 2019;72(2):169–178.
14. Shiraki A, Sakimoto S, Tsuboi K, et al. Evaluation of retinal nonperfusion in branch retinal vein occlusion using wide-field optical coherence tomography angiography. *Acta Ophthalmol.* 2019;97(6):e913–e918.
15. Zheng F, Zhang Q, Motulsky EH, et al. Comparison of neovascular lesion area measurements from different swept-source OCT angiographic scan patterns in age-related macular degeneration. *Invest Ophthalmol Vis Sci.* 2017;58(12):5098–5104.
16. Osaka R, Nakano Y, Takasago Y, et al. Retinal oximetry in branch retinal vein occlusion. *Acta Ophthalmol.* 2019;97(6):e896–e901.
17. Yang JY, You B, Wang Q, Chan SY, Jonas JB, Wei WB. Retinal vessel oxygen saturation in healthy subjects and early branch retinal vein occlusion. *Int J Ophthalmol.* 2017;10(2):267–270.
18. Lin LL, Dong YM, Zong Y, et al. Study of retinal vessel oxygen saturation in ischemic and non-ischemic branch retinal vein occlusion. *Int J Ophthalmol.* 2016;9(1):99–107.
19. Jaulim A, Ahmed B, Khanam T, Chatziralli IP. Branch retinal vein occlusion: epidemiology, pathogenesis, risk factors, clinical features, diagnosis, and complications. An update of the literature. *Retina.* 2013;33(5):901–910.
20. Argon laser photocoagulation for macular edema in branch vein occlusion. The Branch Vein Occlusion Study Group. *Am J Ophthalmol.* 1984;98(3):271–282.
21. Ishibazawa A, Mehta N, Sorour O, et al. Accuracy and reliability in differentiating retinal arteries and veins using widefield en face OCT angiography. *Transl Vis Sci Technol.* 2019;8(3):60.
22. Trinh M, Kalloniatis M, Nivison-Smith L. Vascular changes in intermediate age-related macular degeneration quantified using optical coherence tomography angiography. *Transl Vis Sci Technol.* 2019;8(4):20.
23. Su L, Ji YS, Tong N, et al. Quantitative assessment of the retinal microvasculature and choriocapillaris in myopic patients using swept-source optical coherence tomography angiography. *Graefes Arch Clin Exp Ophthalmol.* 2020;258(6):1173–1180.
24. Ishii H, Shoji T, Yoshikawa Y, Kanno J, Ibuki H, Shinoda K. Automated measurement of the foveal avascular zone in swept-source optical coherence tomography angiography images. *Transl Vis Sci Technol.* 2019;8(3):28.
25. Tang W, Guo J, Liu W, Xu G. Quantitative analysis of retinal and choriocapillary vascular density of multiple evanescent white dot syndrome by optical coherence tomography angiography. *Graefes Arch Clin Exp Ophthalmol.* 2020;258(8):1697–1707.
26. Tang W, Guo J, Liu W, Xu G. Optical coherence tomography angiography of inflammatory choroidal neovascularization early response after anti-VEGF treatment. *Curr Eye Res.* 2020;45(12):1556–1562.
27. Lei J, Durbin MK, Shi Y, et al. Repeatability and reproducibility of superficial macular retinal vessel density measurements using optical coherence tomography angiography en face images. *JAMA Ophthalmol.* 2017;135(10):1092–1098.
28. Lupidi M, Coscas F, Cagini C, et al. Automated quantitative analysis of retinal microvasculature in normal eyes on optical coherence tomography angiography. *Am J Ophthalmol.* 2016;169:9–23.
29. Bland JM, Altman DG. Statistical methods for assessing agreement between two methods of clinical measurement. *Lancet.* 1986;1(8476):307–310.
30. Arthur E, Elsner AE, Sapoznik KA, Papay JA, Muller MS, Burns SA. Distances from capillaries to arterioles or venules measured using OCTA and AOSLO. *Invest Ophthalmol Vis Sci.* 2019;60(6):1833–1844.
31. Michaelson IC. *Retinal Circulation in Man and Animals*. Springfield, IL: Charles C Thomas; 1954.
32. Rehak J, Rehak M. Branch retinal vein occlusion: pathogenesis, visual prognosis, and treatment modalities. *Curr Eye Res.* 2008;33(2):111–131.
33. Petersen L, Bek T. The oxygen saturation in vascular abnormalities depends on the extent of arteriovenous shunting in diabetic retinopathy. *Invest Ophthalmol Vis Sci.* 2019;60(12):3762–3767.
34. Parodi MB, Bandello F. Branch retinal vein occlusion: classification and treatment. *Ophthalmologica.* 2009;223(5):298–305.
35. Campochiaro PA, Bhisitkul RB, Shapiro H, Rubio RG. Vascular endothelial growth factor promotes progressive retinal nonperfusion in patients with retinal vein occlusion. *Ophthalmology.* 2013;120(4):795–802.

36. Michelson G, Warntges S, Baleanu D, et al. Morphometric age-related evaluation of small retinal vessels by scanning laser Doppler flowmetry: determination of a vessel wall index. *Retina.* 2007;27(4):490–498.
37. Im JC, Shin JP, Kim IT, Park DH. Recurrence of macular edema in eyes with branch retinal vein occlusion changes the diameter of unaffected retinal vessels. *Graefes Arch Clin Exp Ophthalmol.* 2016;254(7):1235–1236.
38. Suzuki N, Hirano Y, Tomiyasu T, et al. Collateral vessels on optical coherence tomography angiography in eyes with branch retinal vein occlusion. *Br J Ophthalmol*. 2019;103(10):1373–1379.
39. Daruich A, Matet A, Moulin A, et al. Mechanisms of macular edema: beyond the surface. *Prog Retin Eye Res.* 2018;63:20–68.
40. Lardenoye CW, Probst K, DeLint PJ, Rothova A. Photoreceptor function in eyes with macular edema. *Invest Ophthalmol Vis Sci*. 2000;41(12):4048–4053.
41. Iijima H. Mechanisms of vision loss in eyes with macular edema associated with retinal vein occlusion. *Jpn J Ophthalmol*. 2018;62(3):265–273.
42. Toussaint D, Kuwabara T, Cogan DG. Retinal vascular patterns. II. Human retinal vessels studied in three dimensions. *Arch Ophthalmol.* 1961;65:575–581.
43. Baek SU, Kim YK, Ha A, et al. Diurnal change of retinal vessel density and mean ocular perfusion pressure in patients with open-angle glaucoma. *PLoS One*. 2019;14(4):e0215684.
44. Sun C, Liew G, Wang JJ, et al. Retinal vascular caliber, blood pressure, and cardiovascular risk factors in an Asian population: the Singapore Malay Eye Study. *Invest Ophthalmol Vis Sci.* 2008;49(5):1784–1790.
45. Sampson DM, Gong P, An D, et al. Axial length variation impacts on superficial retinal vessel density and foveal avascular zone area measurements using optical coherence tomography angiography. *Invest Ophthalmol Vis Sci.* 2017;58(7):3065–3072.